Kinetochores Are Transported Poleward along a Single Astral Microtubule during Chromosome Attachment to the Spindle in Newt Lung Cells

Conly L. Rieder*‡ and Stephen P. Alexander* with the technical assistance of Gerald Rupp§

*Wadsworth Center for Laboratories and Research, Empire State Plaza, Albany, New York 12201-0509; ‡School of Public Health, State University of New York at Albany, Albany, New York 12201; and §Department of Anatomical Sciences, State University of New York at Buffalo, Buffalo, New York 14214

Abstract. During mitosis in cultured newt pneumocytes, one or more chromosomes may become positioned well removed (>50 μm) from the polar regions during early prometaphase. As a result, these chromosomes are delayed for up to 5 h in forming an attachment to the spindle. The spatial separation of these chromosomes from the polar microtubule-nucleating centers provides a unique opportunity to study the initial stages of kinetochore fiber formation in living cells. Time-lapse Nomarski-differential interference contrast videomicroscopic observations reveal that late-attaching chromosomes always move, upon attachment, into a single polar region (usually the one closest to the chromosome). During this attachment, the kinetochore region of the chromosome undergoes a variable number of transient poleward tugs that are followed, shortly thereafter, by rapid movement of the chromosome towards the pole. Anti-tubulin immunofluorescence and serial section EM reveal that the kinetochores and kinetochore regions of nonattached chromosomes lack associated microtubules. By contrast, these methods reveal that the attachment and subsequent poleward movement of a chromosome correlates with the association of a single long microtubule with one of the kinetochores of the chromosome. This microtubule traverses the entire distance between the spindle pole and the kinetochore and often extends well past the kinetochore. From these results, we conclude that the initial attachment of a chromosome to the newt pneumocyte spindle results from an interaction between a single polar-nucleated microtubule and one of the kinetochores on the chromosome. Once this association is established, the kinetochore is rapidly transported poleward along the surface of the microtubule by a mechanism that is not dependent on microtubule depolymerization. Our results further demonstrate that the motors for prometaphase chromosome movement must be either on the surface of the kinetochore (i.e., within the corona but not the plate), distributed along the surface of the kinetochore microtubules, or both.

One of the most important aspects of mitosis is the molecular mechanism by which kinetochores attach to and orient toward the poles of the forming spindle. Chromosome micromanipulation experiments and structural studies have clearly demonstrated that this attachment arises from the formation of a birefringent fiber (i.e., a kinetochore fiber [K-Fiber]),[1] composed primarily of microtubules (MTs), that connects each kinetochore with a spindle pole (for review see 50). The acquisition of MTs by the prometaphase kinetochore is also a prerequisite for directed chromosome movement (39, 40). The exact role kinetochore MTs (K-MTs) play in this process is, however, a subject of considerable controversy. It is unclear whether they directly generate and/or transmit the mitotic forces or whether they act as an extrinsic governor (10, 36) to regulate chromosome velocity generated by a mechanistically separate force generator (for reviews see 31, 36, 38, 44, 56).

Although attached chromosomes move continuously throughout the mitotic process, most mitosis research focuses on explaining anaphase motion since at this time chromosome movement is synchronous and predictable in its direction and duration. For example, recent microinjection experiments reveal that K-Fiber MTs are dynamic structures (32, 67), and various models have been proposed to explain anaphase chromosome movement based on these findings (for reviews see 15, 28, 37, 56).

When compared with metaphase and anaphase, relatively little information is available concerning chromosome behavior and spindle structure during prometaphase. It is unclear, for example, how chromosomes become attached to

1. *Abbreviations used in this paper*: DIC, differential interference contrast; IMF, immunofluorescence; K-Fiber, kinetochore fiber; K-MT, kinetochore microtubule; MT, microtubule; NEB, nuclear envelope breakdown; NP, newt pneumocyte; OMDR, optical memory disk recorder.

and oriented on the spindle, how kinetochores acquire their associated MTs, why most attaching chromosomes initially move with a velocity many times greater than that of anaphase chromosomes, or how congression movements are produced and regulated. The lack of information relevant to the mechanism of chromosome transport during prometaphase arises from several factors that complicate the analyses. These include the high density of MTs within the vicinity of chromosomes at the time of nuclear envelope breakdown (NEB), the inability to clearly distinguish primary constrictions (i.e., kinetochore regions) within the overlapping tangle of early prometaphase chromosome arms, and the fact that it cannot be predicted when a prometaphase chromosome will attach to the spindle—only that the process occurs very rapidly during or immediately after NEB (for review see 61).

Early attempts to circumvent the complications inherent in studies of chromosome attachment focused on temporarily delaying MT assembly in prometaphase cells with cold (51), colcemid (70), or nocadazole (7). However, these studies generated controversial and conflicting results that were not amenable to a straightforward interpretation (for review see 46, 50, 66). More recently, Nicklas and Kubai (39) have used the alternative strategy of detaching chromosomes from the spindle of grasshopper spermatocytes by micromanipulation and then placing them 8–10 μm from the spindle. The enhanced spatial separation of such manipulated chromosomes from the "confusing mass of spindle microtubules" (40) enabled these investigators to examine the initial stages of chromosome reattachment using a correlative light and electron microscopy. In all cases, the chromosomes reattached to the spindle and usually moved, kinetochore foremost, towards the metaphase plate. In some cases, renewed movement (i.e., reattachment) could be correlated with the appearance of just a single long MT at the kinetochore.

As a rule, chromosomes that are positioned closer to one pole at the time of NEB usually attach first to that pole and only later acquire a bipolar attachment. This initial monopolar attachment of prometaphase chromosomes is a normal and prevalent feature of astral mitosis (for reviews see 50, 55) and differs substantially from the reattachment of micromanipulated bivalents. In the latter case, the chromosomes generally reattach to both poles simultaneously, and, as a result, movement is directed not toward a pole but toward the metaphase plate (39). Furthermore, the rate of this movement (1.8 μm/min; 35) is very slow relative to the rate of movement measured when chromosomes form an initial attachment to only one pole (up to 24 μm/min; 47, 55).

In living newt pneumocytes (NPs), the spindle poles and the kinetochore regions of chromosomes are clearly visible by light microscopy. These, and other advantages, have made this cell a popular material for studies of mitosis (for review see 52). We have found that occasionally one or more NP chromosomes become positioned, after NEB, $\geqslant$50 μm from the closest spindle pole. Unlike bivalents detached by micromanipulation, these isolated chromosomes ultimately form a monopolar attachment to, and move rapidly toward, the proximal spindle pole. The extreme spatial separation of these chromosomes from the forming spindle provides a unique opportunity to examine the initial stages of K-Fiber formation by high-resolution correlative Nomarski-differential interference contrast (DIC), anti-tubulin immunofluorescent, and electron microscopic methods. The results of this study provide novel insights into the mechanism of K-Fiber formation and force production during mitosis.

Materials and Methods

Cell Culture

Primary cultures of NP from *Taricha granulosa* were prepared as previously described (52). Briefly, small fragments of lung tissue were cultured on 25-mm square coverslips within Rose chambers in 0.5× L-15 medium supplemented with 10% FCS, 5% whole-egg ultrafiltrate, 5 mM Hepes (pH 7.1), and antibiotics. When incubated at 23–26°C, mitotic cells could be found within the pneumocyte monolayers after 7–10 d in culture.

Light Microscopy

For routine observations, mitotically active Rose chamber cultures were examined with an inverted microscope (Diaphot-TMD; Nikon Inc., Garden City, NY) equipped with phase-contrast optics. When a cell was located for subsequent high-resolution study, the Rose chamber was quickly dismantled, and the culture-containing coverslip was remounted with VALAP in culture media on a McGee-Russell and Allen (23) microperfusion chamber. Once mounted in these chambers, the cultures remained mitotically active for up to 3 d.

Cells were observed within the microperfusion chambers with a Microphot-FX microscope (Nikon Inc.) equipped with DIC (40×; NA = 0.85) and phase-contrast (40×; NA = 0.65) optics. Heat-filtered green (546 nm) light, obtained from a quartz halogen or tungsten lamp, was used to illuminate the cells. Cell irradiation during time-lapse video microscopy was minimized, when an optical memory disk recorder (OMDR) was used as the recorder, by shuttering the light source with a Uniblitz shutter (Vincent Assoc., Rochester, NY) driven by the same XT-class computer (see below) controlling the OMDR. Analogue images were acquired with a video camera (70 Newvicon; Dage-MTI Inc., Wabash, MI) coupled to a digital image processor (DVS 3000; Hamamatsu Phototonics K. K., Hamamatsu City, Japan). The raw and digitally processed images were viewed simultaneously by feeding the camera output through a primary monitor before sending it to the digital processor, recording device, and secondary monitor. The digitally processed images were recorded with either a 1/2" time-lapse VCR or an OMDR (TQ 2025F; Panasonic Industrial Corp., Secaucus, NJ) operated in a time-lapse mode under control of an IBM-compatible XT-class microcomputer with custom-designed software (Laserbase; SMI Systems, Ft. Lauderdale, FL). With computer control of the OMDR we were able to enter both the desired recording rate and the interval of illumination for each frame, with each OMDR recorded frame being an average of eight real-time frames. Typically, illumination commenced 0.25 s before a frame was recorded by the OMDR and ceased 0.1 s after, giving a total irradiation time of ~0.75 s per frame.

For immunofluorescence (IMF) microscopy, selected mitotic NPs were followed within perfusion chambers before and after perfusion with 1% glutaraldehyde in PHEM buffer (pH 7.2; 60). Approximately 1 min later, the chamber was removed from the microscope stage and quickly disassembled, and the culture-containing coverslip was immersed in a Petri containing 0.5% glutaraldehyde and 0.5% Triton X-100 in PHEM buffer. After 4 min in this fixation/permeabilization solution, the culture was fixed for 15 min with 0.1% glutaraldehyde in PHEM buffer. The preparation was then washed in PHEM buffer (three changes; 5 min each) and reduced within a Coplin jar by treatment with 0.5 mg/ml $NaBH_4$ in PHEM buffer (three changes; 5 min each). The culture was next washed in PBS (three changes; 5 min each) and blocked at 37°C for 30 min in 5% FBS and 0.2% Tween-20 in PBS. It was then incubated, without washing, in a monoclonal antibody against β-tubulin (TU-27; kindly provided by L. Binder, University of Alabama, Birmingham, AL) at 37°C for 30–45 min. After washing in PBS, the culture was treated with a rhodamine-conjugated goat anti-mouse IgG (Sigma Chemical Co., St. Louis, MO) at 37°C for 30 min. Finally, it was washed in PBS and mounted on a slide in PBS/glycerol (pH 7.8) containing *N*-propyl gallate.

Cells processed for the indirect IMF localization of MTs were examined with an Optiphot microscope (Nikon Inc.) equipped with 40× and 100× phase-contrast objectives (NA = 1.3). Fluorescent and phase-contrast images were photographed on XP-1 film (Ilford Ltd., Basildon, Essex, England) using an ASA setting of 1,600 and an automatic exposure system

(UFX; Nikon Inc.). This film was then commercially developed by C-41 processing. Images from video recordings were photographed on Plus X film (Eastman Kodak Co., Rochester, NY) using a freeze-frame video recorder (Polaroid Corp., Cambridge, MA). This film was subsequently processed in Rodinal.

Electron Microscopy

Cells followed within the perfusion chambers were fixed for electron microscopy by one of two methods, the choice of which depended on whether the cell would be first processed for IMF microscopy. Cells not destined for antibody staining before embedding were fixed in phosphate-buffered glutaraldehyde and osmicated as previously detailed (53). Cells to be processed initially for IMF were fixed in PHEM-buffered 1% glutaradehyde and stained as described above. After fluorescence microscopy, the preparation was removed from the slide and washed in PBS. It was then postfixed in 1% OsO_4 in 0.5 M phosphate buffer for 15 min at 4°C, washed in distilled H_2O, and stained en bloc with 1% aqueous uranyl acetate for 2 h. Cultures fixed by either of these two methods were dehydrated in a graded series of ethanols and flat embedded in Epon-Araldite. The cell of interest was then excised from the embedment, glued to an Epon peg, and cut serially into 0.25-μm-thick or 80-nm-thick sections. The ribbons of serial sections were mounted on Formvar-coated slot grids and stained in uranyl acetate and lead citrate. Thick sections were viewed and photographed in the Wadsworth Center's (Albany, NY) AEI high voltage electron microscope operated at 800 kV, while thin sections were viewed and photographed at 80 kV on a Philips Electronic Instruments, Inc. (Mahwah, NJ) 301 electron microscope.

Computer-aided reconstructions from serial thin sections were made using STERECON, a system developed at the Albany high-voltage electron microscope facility (21). Briefly, prints of serial 80-mm sections were enlarged to a final magnification of 13,000×. For each section, profiles were drawn on clear acetate sheets outlining the chromosomes, kinetochores, mitochondria, and other spindle constituents. The sheets were then aligned by best fit of the profiles. These profiles were entered into a computer (VAX-780/750; Digital Equipment Corp., Maynard, MA) using a digitizing tablet, and a profile-stack reconstruction was made. After the best viewing angle was established by inspecting stereo pairs of the profile stacks, the data was read into MOVIE.BYU (Brigham Young University, Salt Lake City, UT), and shaded, solid-model views were made. The resolution in the x- and y-axes of each three-dimensional reconstruction was equivalent to that obtainable by standard transmission electron microscopy, but in the z-axis it was limited to the section thickness (i.e., 80 nm).

Motion Analysis

Frame-by-frame analysis of individual chromosome movement was conducted on OMDR-recorded images reprocessed through the digital image processor (DVS 3000; Hamamatsu Phototonics K. K., Oak Brook, IL). The digital image processor has a distance mode that displays x- and y-coordinates for two moveable cursors and simultaneously calculates the distance between them. This system was calibrated using the 0.62-μm frustule spacing of the diatom *Pleurasigma angulatum* under the same optical conditions. The positions of the pole and kinetochore (or edge of the primary constriction in cases where the kinetochore was not clearly visible) were tracked manually by positioning the cursors in each frame. When the pole-to-kinetochore distance allowed, measurements were conducted in the zoom mode which enables a 2× magnified image to be used in distance measurements. For each frame, the x- and y-pixel coordinates of both the spindle pole and the kinetochore, together with the calculated distance, were entered manually into a Lotus spread sheet (Lotus Development Corporation, Cambridge, MA) for calculations. The resulting data was then imported into Harvard Graphics (Software Publishing Corp., Mountain View, CA) for graph plotting.

Results

Origin of Chromosomes Delayed in Attaching to the NP Spindle

As in other types of astral spindles (for reviews see 50, 55), the order in which chromosomes attach to the NP spindle is dictated by their distances from the spindle poles at the time of NEB (Fig. 1). As a rule, chromosomes closer to the poles are the first to attach. The prevalent behavior pattern of these chromosomes is to initially monoorient and move towards the nearest pole before achieving a bipolar orientation. In most NPs, the poles begin separating, along the dorsal surface of the nuclear envelope, just before NEB. As a result,

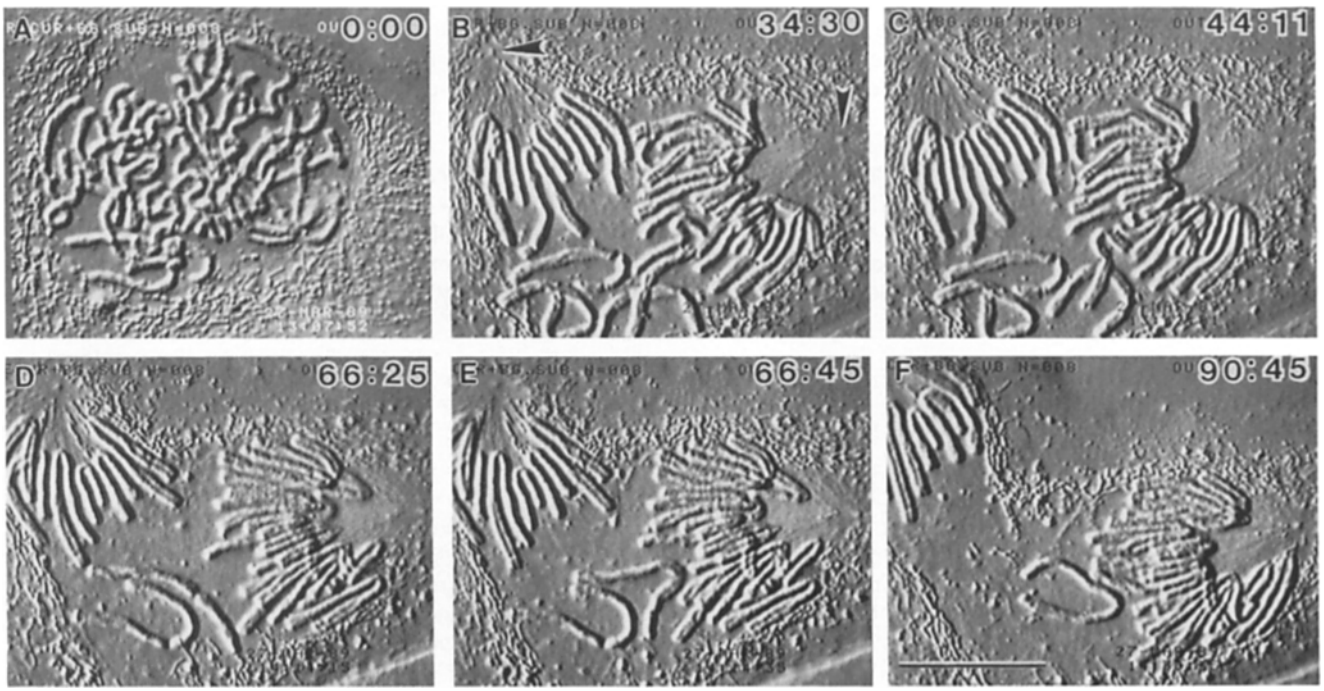

Figure 1. Selected DIC videomicrographs of an NP undergoing an anaphase-like prometaphase. Time (in min:s) is noted in the upper right corner of each micrograph. This cell contains a number of unattached chromosomes between the separating spindle poles (*B, arrowheads*). Over a 90-min period, all of these chromosomes attached to the right-hand pole. Note that those chromosomes closest to the pole are the first to attach. Bar, 25 μm.

when NEB occurs the separating spindle poles are in the immediate vicinity of the chromosomes, the central spindle is well developed, and most chromosomes attach to one or both poles within the first 5 min of prometaphase. During this time, the area containing the forming spindle is crowded with chromosomes and it is seldom possible to continuously follow the kinetochore region of a chromosome from its initial point of attachment through its subsequent movement into the pole, even though this movement may cover only a few micrometers. Our study was therefore conducted on chromosomes far from a pole and significantly delayed (>20 min) by natural events in attaching to the spindle. Since these chromosomes are always temporally and spatially separated from the attachment of other chromosomes, they can be unambiguously followed for considerable distances during the attachment process. The 22 chromosomes in *Taricha* are either metacentric or submetacentric and each carries a prominent kinetochore-associated primary constriction that is clearly visible in the living cell (Fig. 1). As a result, chromosomes delayed in their attachment can be readily differentiated from akinetic chromosome fragments that never attach to the spindle.

Chromosomes that are delayed in attaching to the NP spindle are generated by several natural routes, all of which produce an exaggerated separation between the chromosome(s) and closest spindle pole during the early stages of prometaphase. In ~2% of NPs, the replicated centrosomes separate precociously during mid rather than late prophase. Under these conditions centrosome separation is well advanced at the time of NEB, none of the chromosomes acquire a bipolar orientation, and an anaphase-like prometaphase ensues as previously described by Bajer (1). During this process, most chromosomes quickly monoorient to the closest pole as the poles continue to separate. However, ~20% of these cells possess chromosomes, situated between the two migrating spindle poles at the time of NEB, that are considerably delayed in their attachment (Fig. 1). In general, the farther a chromosome is from the closest pole, the longer it is delayed in attaching to that pole (Fig. 1).

In rarer instances (>1%), centrosome separation in NPs is initiated at the normal time but it occurs along a lateral edge of the nucleus, or even well removed from the nucleus, rather than along its dorsal surface. Unlike anaphase-like prometaphase cells, the chromosomes on the side of the nucleus facing the separating poles rapidly acquire attachments to both poles and bipolarize the forming spindle. However, those chromosomes more distal to the forming spindle—i.e., those on the opposite side of the nucleus—are frequently delayed in attaching (data not shown).

Finally, in some cells the centrosomes fail to separate or begin to separate well after NEB. Under these conditions, a permanent or transient monopolar spindle is produced in which those chromosomes more distal to the single polar area can be delayed in their attachment (data not shown).

We analyzed our data to determine the kinetochore-to-pole distance at that time when a chromosome, delayed in attaching to the spindle, formed its initial attachment (Fig. 2). This analysis indicates that chromosomes are not usually delayed (i.e., for a longer duration than our definition of ~20 min) in attaching to the spindle if they are within 30 μm of the closest polar area at the time of NEB and that attachment rarely if ever occurs when a chromosome is >50 μm from a pole. Indeed, although chromosomes could be found in anaphase-like prometaphase cells that are >50 μm from the closest pole, these chromosomes were not seen to attach until they achieved a position closer than that to a pole, a process that sometimes required up to 5 h. During this time, the chromosome-to-pole distance was reduced either by random movement of the chromosome towards the pole, generated by Brownian forces and cytoplasmic currents, or by movement of the pole closer to the chromosome. In unusual instances (encountered twice), a chromosome became trapped so far from a polar area (e.g., within a false interzone; see reference 1) that it never attached to the spindle.

A detailed kinetic analysis of prometaphase chromosome movements in NPs will be described elsewhere (Alexander, S. P., and C. L. Rieder, manuscript in preparation). In summary, during attachment the kinetochore region of the chromosome undergoes a variable number of transient poleward tugs that are followed, shortly thereafter, by rapid movement of the chromosome towards the pole.

Structural Analysis of Chromosome Attachment

Our structural analysis of chromosome attachment was conducted primarily, but not exclusively, on anaphase-like prometaphase cells. Chromosomes delayed in their attachment to the spindle are most frequently encountered in such cells which, as described below, lack a central spindle. Since the spindle poles in these cells can wander great distances apart (1), unattached chromosomes are frequently found ≥50 μm from the closest pole. As a result, when attachment finally occurs it generally does so in an environment of extremely low MT density.

Indirect anti-tubulin IMF reveals that in all cases anaphase-like prometaphase cells contained two well-separated astral MT arrays within cytoplasm otherwise devoid of MTs (Figs. 3 and 4). One or more monooriented chromosomes were associated with each aster. The distal (i.e., plus end) termination points of those individual MTs within 20 μm of the aster center could not be determined with certainty because of high MT density. Consequently, the average MT length within a given aster could not be calculated. In contrast, the density of MTs 25–30 μm distal to the astral center was low relative to that proximal to the center, and their distal ends were therefore clearly visible (Fig. 3 *C*). To estimate the maximum length that MTs can attain in these asters, we measured the distal termination points of the 35 longest MTs in each of three asters. In each case only those MTs on the chromosome side of the aster were chosen for analysis. That the thin fluorescent lines we analyzed actually corresponded to individual astral MTs has been convincingly argued by others (41) and was subsequently confirmed by our ultrastructural analyses (see below). Assuming that each of these MTs was continuous along its length and connected to the astral center, we found that 13% were >40 μm in length, 41% were between 34 and 39 μm in length, and 48% were between 26 and 33 μm in length. The longest MT in each of these three asters was 42, 43, and 47 μm, respectively.

When examined by anti-tubulin IMF the kinetochore regions on chromosomes that had not attached to the spindle were free of MTs (Fig. 4; $n = 16$ chromosomes in 10 cells). As demonstrated below, our IMF procedure is clearly capable of revealing individual kinetochore-associated MTs had

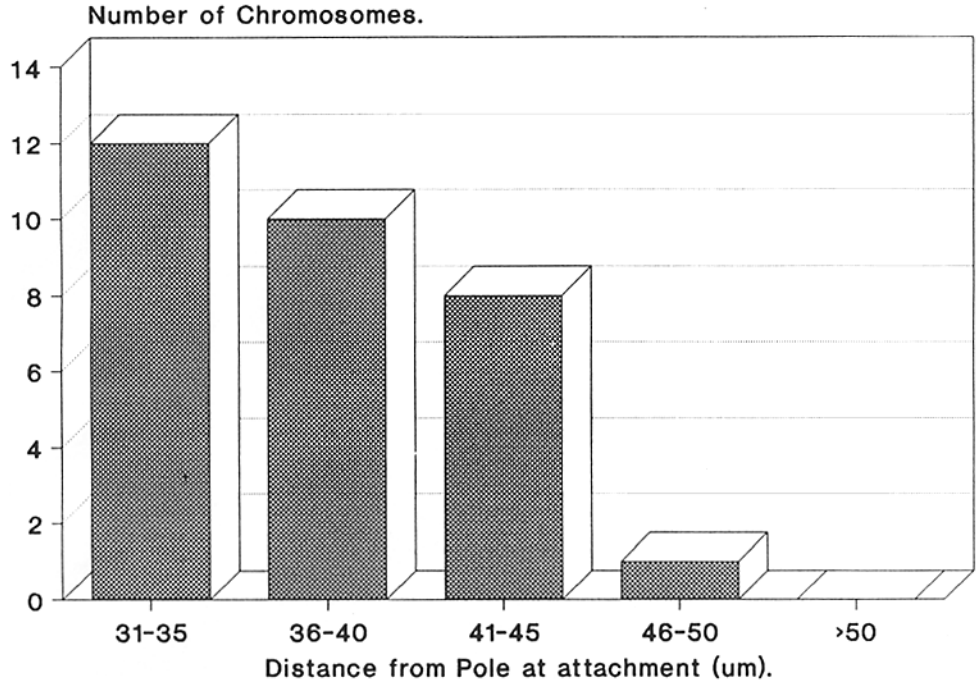

Figure 2. Histogram showing the number of delayed-attaching chromosomes vs. distance from the pole at the time of attachment. Chromosomes were not seen to attach if they were located >50 μm from the closest pole. By contrast, chromosomes located ⩽30 μm from the closest pole were not significantly delayed in attaching to the spindle.

they been present. Since all of the MTs within these cells were associated with an aster and their attached chromosomes (Figs. 3 and 4) and because astral MTs were seldom >50 μm long (see above) and their density progressively decreased with increasing distance from the astral center, the proximity of an unattached chromosome to even a single astral MT clearly depended on how far the chromosome was from the closest pole. Indeed, no MTs were seen in the vicinity of chromosomes well removed from the asters (Fig. 4).

The absence of kinetochore-associated MTs on unattached chromosomes was confirmed by serial section ultrastructural analyses of cells fixed either by conventional methods (Fig.

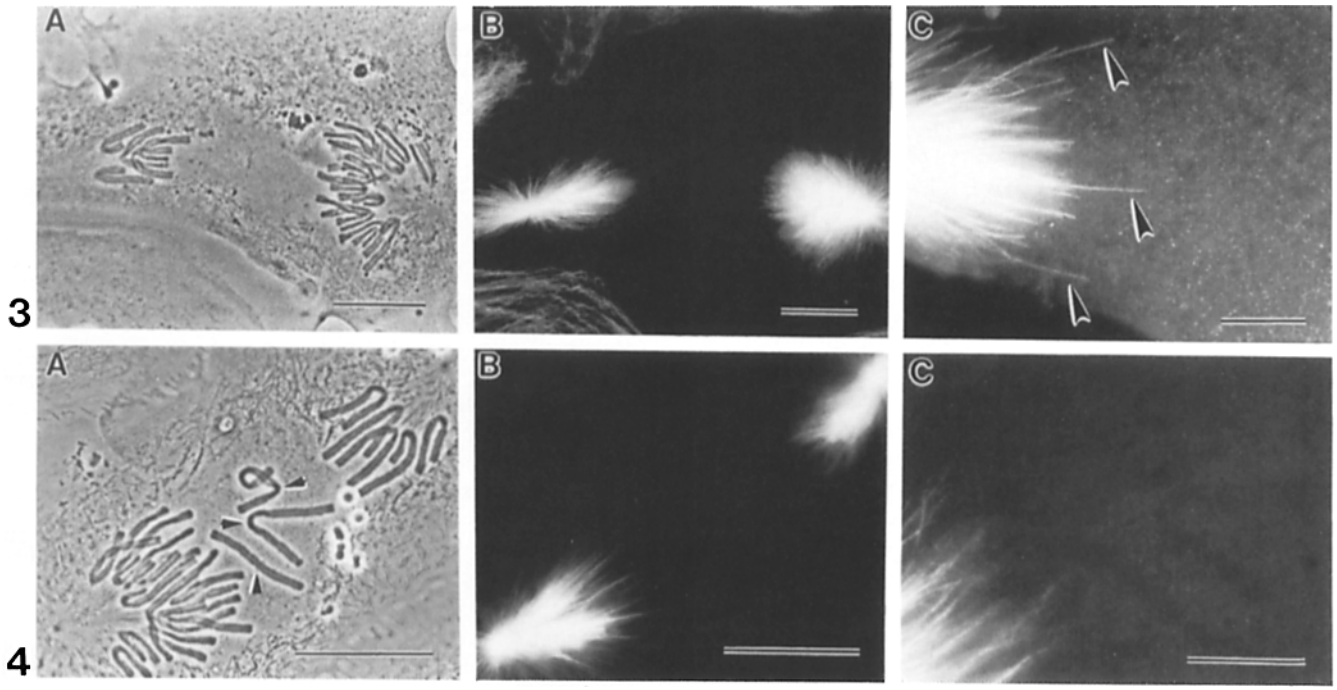

Figures 3 and 4. (Fig. 3) Phase-contrast (*A*) and anti-tubulin immunofluorescent (*B* and *C*) micrographs of an anaphase-like prometaphase NP. Note that MTs are not present in the region between the well-separated asters (*B*) and that each aster contains a population of long MTs (*C*, *arrowheads*). Bars: (*A* and *B*) 25 μm; (*C*) 10 μm. (Fig. 4) Phase-contrast (*A*) and anti-tubulin immunofluorescent (*B* and *C*) micrographs of an anaphase-like prometaphase NP that contains three unattached chromosomes (*A*, *arrowheads*) between the well-separated asters. Note that MTs are not seen to be associated with the unattached chromosomes when examined at either low (*B*) or high magnification (*C*). The micrograph in *C* was printed to reveal the unattached chromosome outlines. Bars: (*A* and *B*) 25 μm; (*C*) 10 μm.

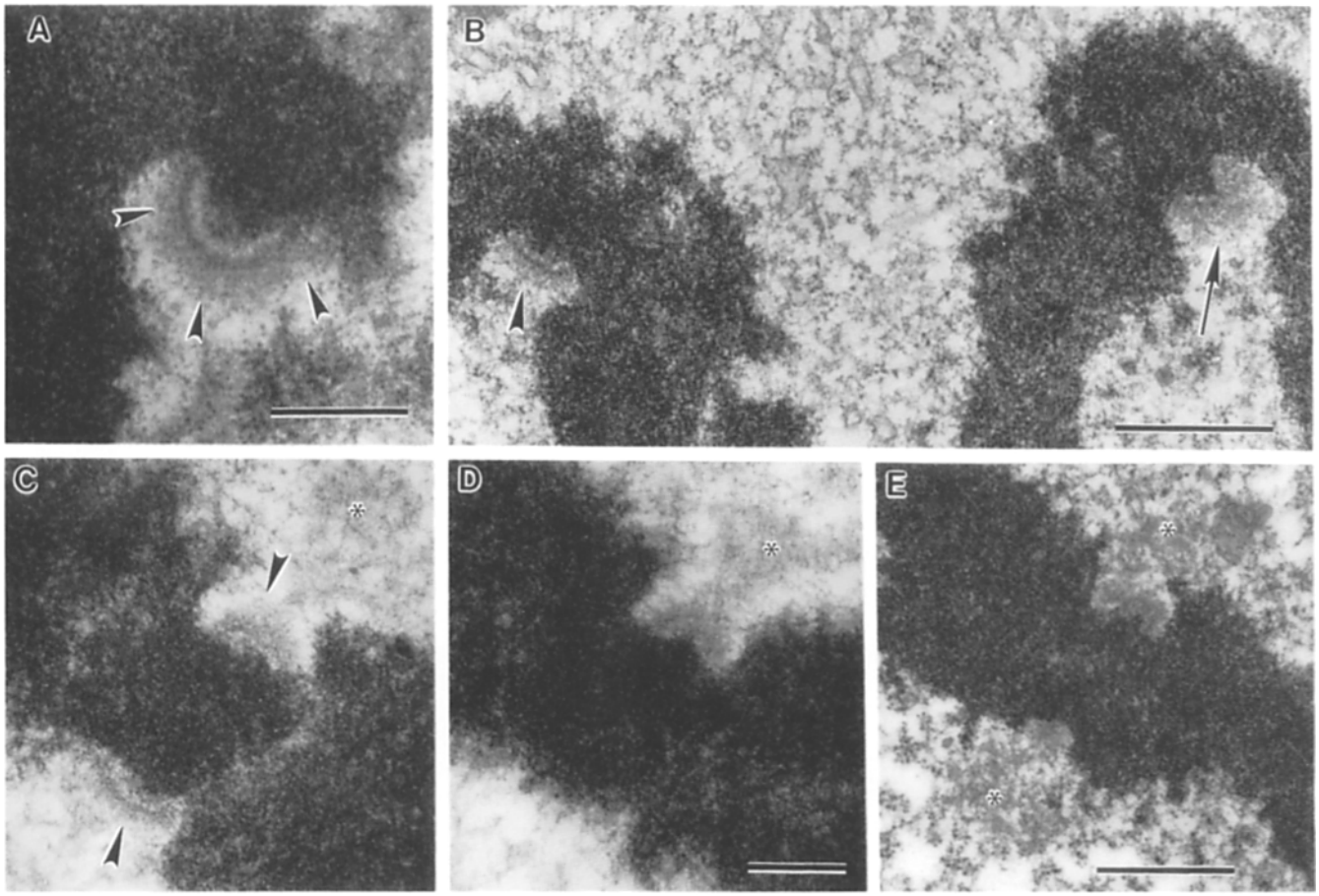

Figure 5. (*A*) High-voltage electron micrograph of an 0.25-μm-thick section through the unattached kinetochore on a monooriented NP chromosome. The kinetochore plate and its associated corona (*arrowheads*) are clearly visible in this plane of section. (*B*) Electron micrograph of an 80-nm-thick section cut through the distal kinetochores of two monooriented chromosomes. One of these kinetochores is cut to reveal the plate structure (*arrowhead*), while the other (*arrow*) is sectioned tangentially and appears as a patch of fibrillar material. (*C* and *D*) High-voltage micrographs of serial 0.25-μm-thick sections through the primary constriction of an unattached chromosome. Both kinetochores (*C*, *arrowheads*) lack associated MTs. Asterisks note extensive corona material. (*E*) Electron micrograph of an 80-nm-thick section through the primary constriction of an unattached chromosome. Note the loose organization of the corona material and the extent to which it radiates from the primary constriction. Bars: (*A*) 0.5 μm; (*B* and *E*) 1 μm; (*C* and *D*) 0.5 μm.

5) or fixed for IMF and then subsequently embedded (data not shown). In the appropriate plane of section, the distal (unattached) kinetochore on a monooriented NP chromosome consisted of a convex plate, 0.35–0.50 μm in diameter, which was separated from the adjacent chromatin by a narrow electron-translucent zone (Fig. 5, *A* and *B*). In these views, a well developed and lighter staining fibrillar corona was associated with and radiated from the surface of the plate (Fig. 5 *A*, *arrowheads*). However, the distal kinetochore of a monooriented chromosome was rarely sectioned in such an opportune plane and usually appeared instead as a loosely-organized, roughly circular patch of fibrillar material that stained less electron opaque than the adjacent chromatin (Fig. 5 *B*, *arrow*). The structure of each sister kinetochore on an unattached NP chromosome typically resembled that of the unattached kinetochore on a monooriented chromosome (Fig. 5, cf. *A–E*). However, the corona material on the distal kinetochore of a monooriented chromosome rarely extended >0.25 μm from the kinetochore plate (Fig. 5 *A*). By contrast, the corona material on sister kinetochores of a nonattached chromosome often extended 0.5–1 μm from the kinetochore plate and, as a result, appeared much more diffuse (Fig. 5, *C–E*).

To determine how MTs were distributed during the initial stages of chromosome attachment, we mounted coverslips containing primary cultures of NPs on perfusion chambers and followed cells containing unattached chromosomes with the video microscope. At some point after the kinetochore initiated its rapid poleward movement, the cell was fixed by perfusion. Because this movement is very rapid it was easily detected in real time. We were not always able to keep the chromosome in focus throughout fixation. However, in those cases where we were able to maintain focus all movement within the cell abruptly ceased 10–15 s after initiating the perfusion. Frame-by-frame analyses of these records (Fig. 6, *A–F*) revealed that most of this time is required for the fixative to reach the cell and that once it did so all motion stopped within 1–2 s.

During the early stages of this study, we videotaped five cells containing late-attaching chromosomes and then fixed these cells, at various times after chromosome attachment, for serial section electron microscopic analyses. One of the

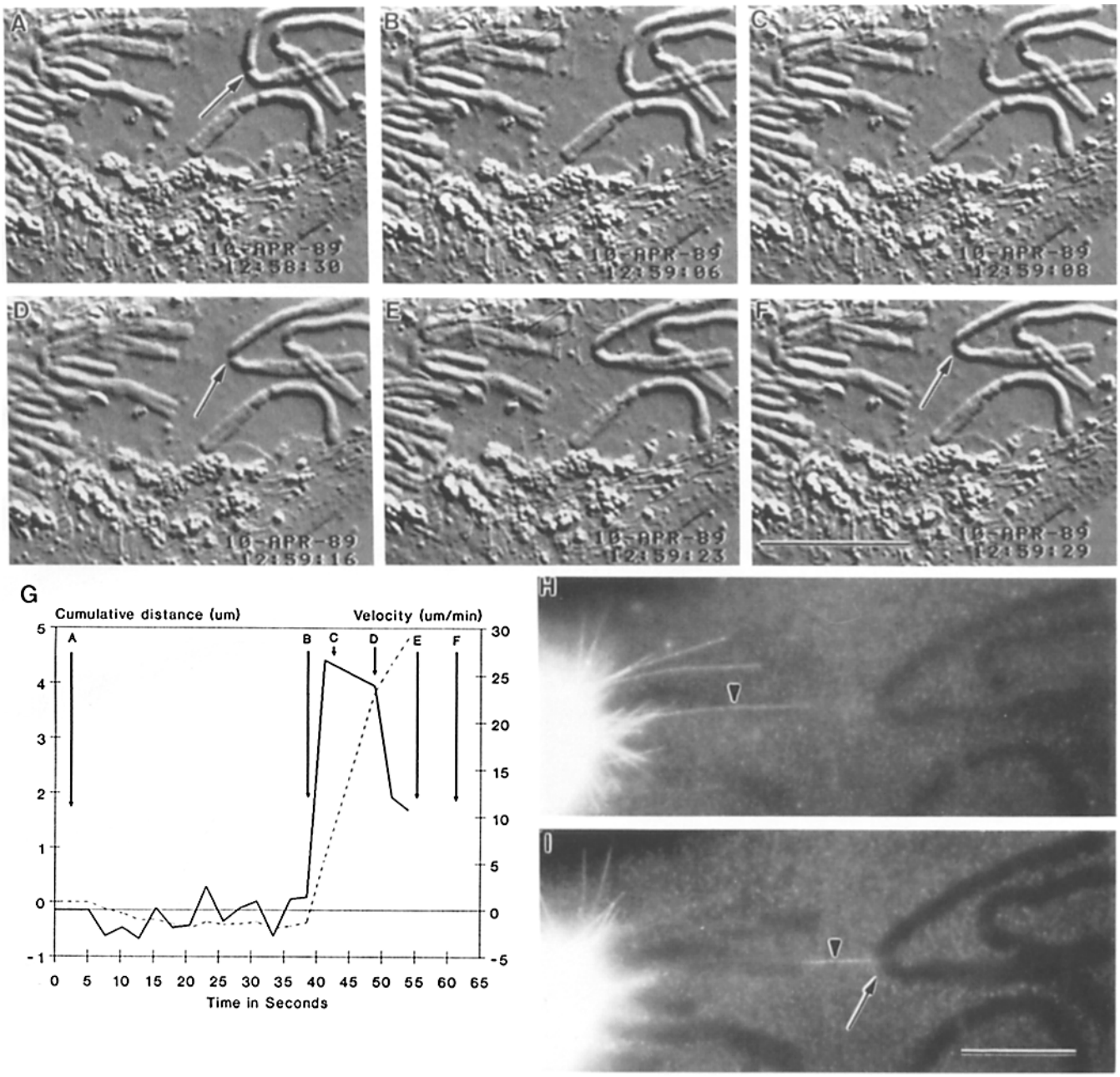

Figure 6. (*A–F*) Selected DIC videomicrographs, from a time-lapse recording, of a chromosome (*A*, *arrow*) being fixed by perfusion immediately after attachment and the initiation of poleward movement. Time (h:min:s) is visible in the bottom right-hand corner of each micrograph. The first evidence of attachment occurs in *B*, at which time the perfusion was initiated. The chromosome continues to move (*C* and *D*) until the fixative reaches the cell (*E*) 17 s later (cf. *E* and *F*). The velocity and net poleward movement of this chromosome, until the point of fixation, is plotted in *G*. The lettered arrows within this plot note the corresponding frames pictured in *A–F*. This cell was subsequently processed for the indirect IMF localization of MTs as shown in *H* and *I*. These two fluorescent micrographs, which were taken at different focal planes, reveal that the chromosome is attached to the spindle pole by a single long MT (*H* and *I*, *arrowheads*) that terminates at the primary constriction of the chromosome (*I*, *arrow*). Bars: (*A–F*) 20 μm; (*H* and *I*) 10 μm.

two chromosomes fixed 20–30 s after attachment had only a single MT in its vicinity, and this MT was laterally associated with, and extended well past, the kinetochore located on the ventral surface of the chromosome (Figs. 7 and 8). The other chromosome possessed two MTs in the vicinity of its primary constriction, and both of these appeared to terminate near or on the kinetochore facing the growth substrate (data not shown). The attaching chromosomes in the remaining three cells were closer to the pole at the time of fixation. In each case, the attached kinetochore possessed between four and seven MTs, while the nonattached kinetochore was free of MTs. Although some of these MTs terminated on or near the kinetochore, the majority terminated well distal to this structure after either passing through it or associating with its periphery (Figs. 9 and 10).

Our same-cell correlative light and electron microscopic

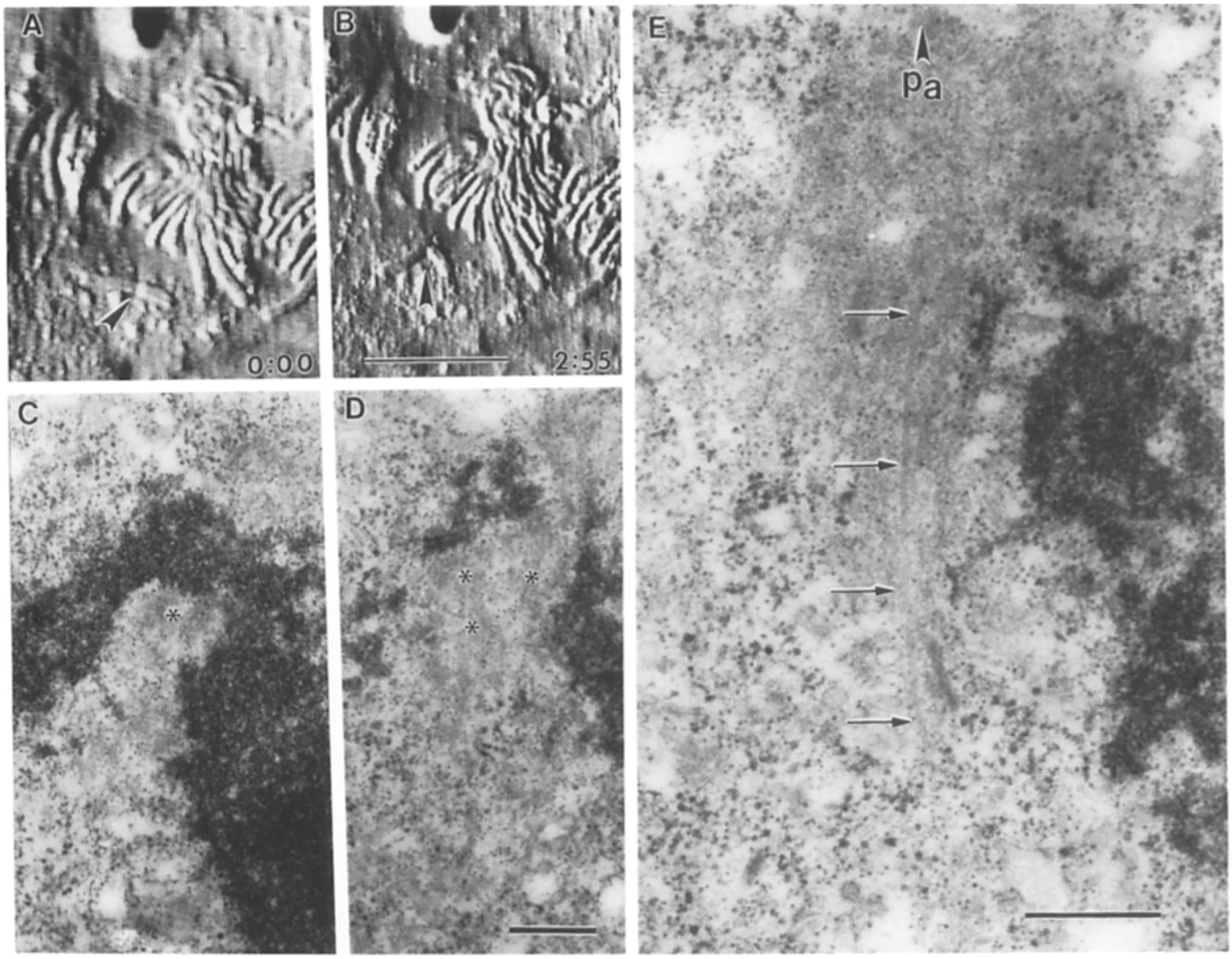

Figure 7. (*A* and *B*) Selected DIC videomicrographs of an NP chromosome (*arrowheads*) before (*A*) and after attachment and fixation (*B*). Time (min:s) is at the bottom right corner of each micrograph. (*C–E*) Electron micrographs of sections three, five, and seven from a serial series cut through the chromosome noted by the arrowhead in *B*. The only MT in the vicinity of this chromosome is noted by the arrows in *E*. This MT is associated with, and extends well past, one of the kinetochores (*C* and *D*, *asterisks*). Compare this figure with Fig. 8. *Pa*, direction of the polar area. Bars: (*A* and *B*) 25 μm; (*C* and *D*) 0.5 μm; (*E*) 0.5 μm.

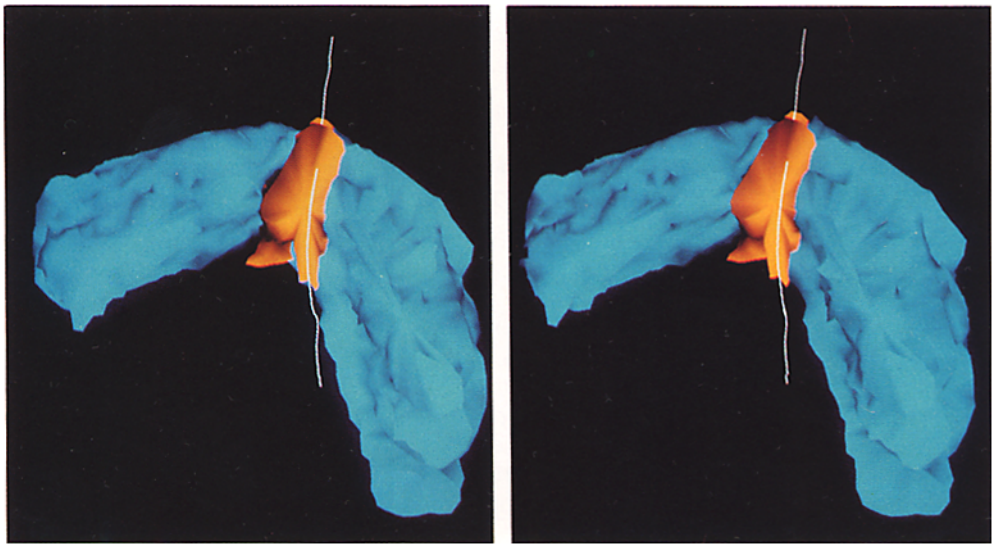

Figure 8. Three-dimensional reconstruction, from serial thin sections, of the chromosome noted by the arrowhead in Fig. 7 *B*. For display clarity, only the active ventral kinetochore was included in the reconstruction. In this stereo pair, the only MT in the vicinity of this chromosome can be seen to associate with and extend well past this kinetochore.

Figure 9. DIC (*A* and *B*) and phase-contast (*C*) micrographs of a late-attaching chromosome (*arrow*) attaching to a monopolar NP spindle. The chromosome attached shortly after the micrograph in *A*, and the cell was fixed at *B*. The cell is then pictured, after embedding in plastic, in *C*. Time (h:min) is at the bottom right corner of each micrograph. Compare this with Fig. 10. Bar, 25 μm.

data indicated that the initial attachment and poleward movement of a chromosome in NPs arises from the acquisition of a single MT by one of the kinetochores on the chromosome. Subsequent observations revealed that this MT could be readily visualized in our preparations by anti-tubulin IMF. We therefore fixed an additional 10 cells containing chromosomes delayed in their attachment, ~30 s after they began their rapid poleward movement. These cells were then processed for the indirect IMF localization of MTs and, in some instances, subsequently embedded for a more laborious serial section electron microscopic analysis. In six cells, only a single MT was found to be associated with the primary constriction (i.e., kinetochore region) of the chromosome attaching to the spindle at the time of fixation (Figs. 6 and 11). That these kinetochore regions were moving poleward at the time of fixation was clearly evident from the time-lapse OMDR sequences (Fig. 6, *A–G*, and Fig. 11, *A–D* and *G*). In all cases, this MT ran continuously from within the aster to or beyond the primary constriction of the chromosome. In three of these cells, the distal end of this MT extended well past the primary constriction (Fig. 11). However, in the other three cells it appeared to terminate on or near this structure (Fig. 6). Although the proximal ends of these MTs could not be determined, they were well within the asters.

In the remaining four cells, two or more MTs were found near the kinetochore region of the attaching chromosome (Fig. 12). In all of these cells, one or more of these MTs extended well past the primary constriction while the remainder terminated at or near this structure.

Five of the ten cells described above were embedded, after IMF microscopy, for a subsequent serial section ultrastructural analysis. In every case, each fluorescent line seen to be associated with a primary constriction by IMF corresponded, at the electron microscope level, with an individual kinetochore-associated MT. A single astral MT, that appeared by IMF to extend well past the primary constriction, could always be followed in serial sections from within the aster to its termination distal to the kinetochore (Fig. 11, *F*, *H*, and *I*). Similarly, those individual astral MTs, which appeared by IMF to terminate on the primary constriction, could be tracked to the kinetochore. However, because the plane of section was invariably unfavorable we were not, in these latter cases, able to differentiate whether the MT terminated in the corona material or the kinetochore plate (data not shown).

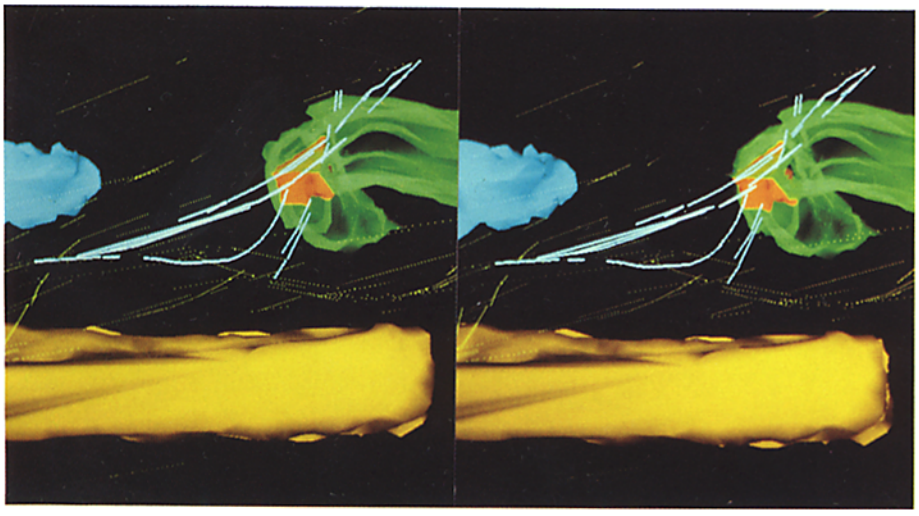

Figure 10. Three-dimensional reconstruction, from serial thin sections, of the chromosome noted by the arrow in Fig. 9. For display clarity only the active attached kinetochore is included in the reconstruction. Non-K-MTs are represented by dotted lines, while K-MTs appear as solid lines. Stereo viewing of this reconstruction reveals that four of the five MTs associated with this kinetochore extend through the kinetochore material. The only MT that terminates in the kinetochore appears bent.

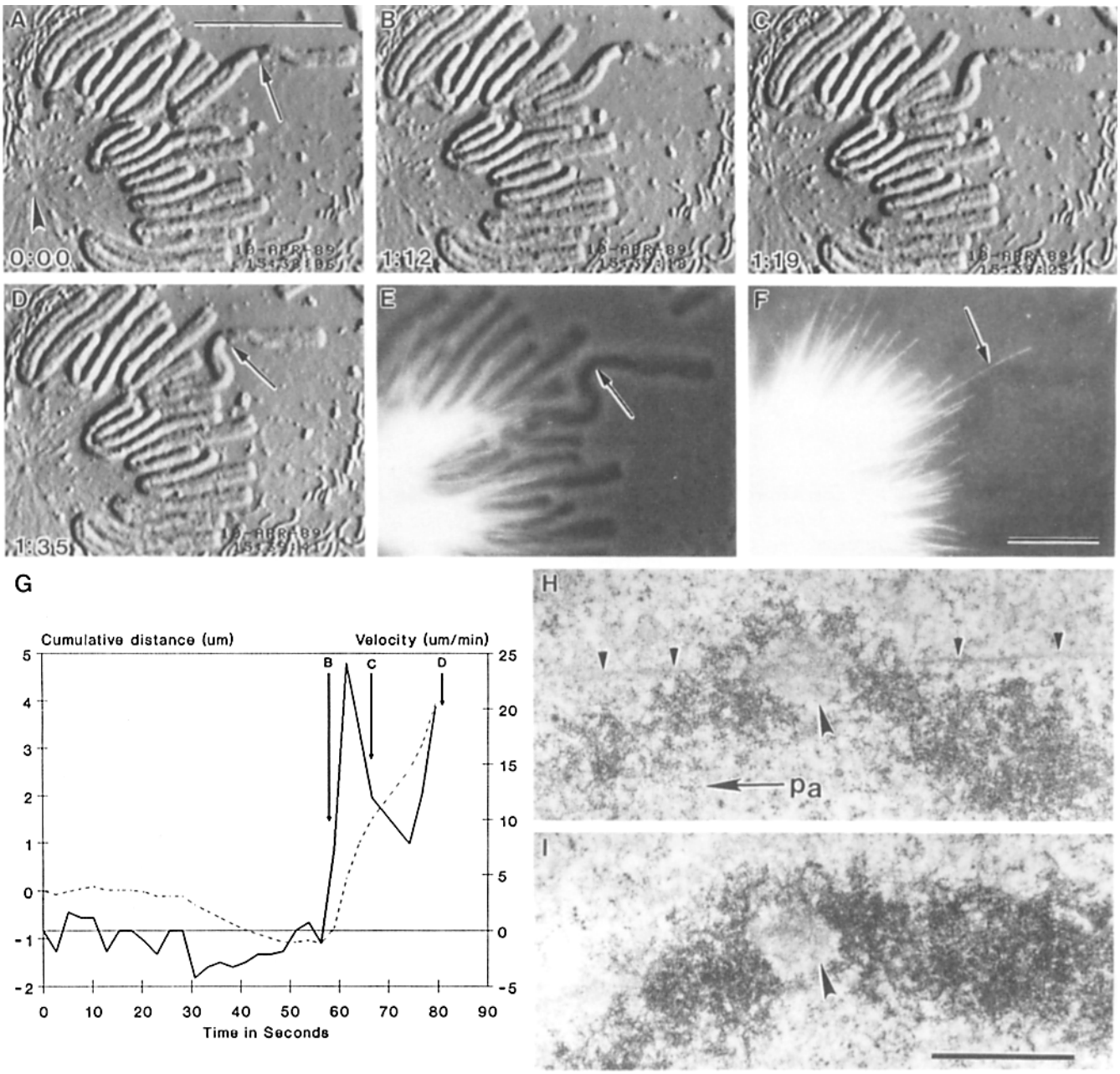

Figure 11. (*A–D*) Selected DIC videomicrographs, from a time-lapse recording, of a chromosome (*A*, *arrow*) being fixed by perfusion immediately after attaching and initiating its poleward movement. The polar area (*A*, *arrowhead*) is clearly visible throughout the series. Time (min:s) is noted in the bottom left-hand corner of each micrograph. Attachment occurs in *B*, and the primary constriction of the chromosome continues to move poleward (*C*) until the fixative reaches the cell, 23 s later (*D*). This cell was then processed for the indirect IMF localization of MTs as shown in *E* and *F*. These two micrographs were printed to reveal the attaching chromosome (*E*, *arrow*) and the MT associated with its primary constriction (*F*, *arrow*). Note that this MT can be followed continuously from within the aster to its termination well past (i.e., distal to) the primary constriction. A plot of this chromosome's motion until fixation, in velocity (*solid line*) and cumulative poleward distance moved (*dashed line*), is shown in *G*. The lettered arrows within this plot correspond to the frames pictured in *B–D*. This cell was subsequently embedded and sectioned for electron microscopy. Serial electron micrographs (*H* and *I*) confirm that the thin fluorescent line noted by the arrow in *F* corresponds to a single MT (*H*, *small arrowheads*) that is associated with, and extends well past, the surface of the kinetochore (*H* and *I*, *large arrowhead*). *Pa* (in *H*), direction of the polar area. Bars: (*A–D*) 20 μm; (*E* and *F*) 10 μm; (*H* and *I*) 1 μm.

Discussion

Our results are relevant to the formation and structure of K-Fibers in vertebrate cells and the mechanism by which chromosomes are transported during prometaphase.

The Formation of K-Fibers

The longstanding controversy concerning the origin of K-Fibers, and their associated MTs (K-MTs), remains to be clearly resolved (for reviews see 26, 37, 50, 56). The more contem-

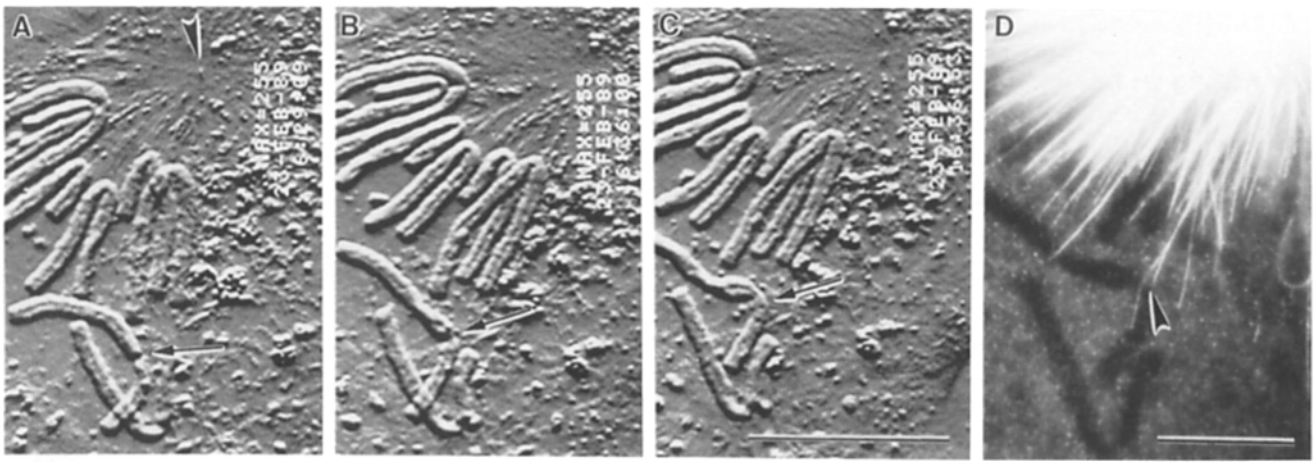

Figure 12. (*A–C*) Selected DIC videomicrographs, from a time-lapse recording, of a chromosome (*A–C, arrows*) being fixed by perfusion shortly after initiating its poleward movement. Time (h:min:s) is noted at the upper right-hand side of each micrograph. Attachment occurs immediately after the frame in *A*, and the cell is fixed by the frame in *C*. This cell was processed for the indirect IMF localization of MTs (*D*). Fluorescent microscopy (*D*) subsequently revealed that the kinetochore region of this chromosome (*D, arrowhead*) possessed two associated MTs: one terminates at the primary constriction, while the other extends well past this structure. Bars: (*A–C*) 20 μm; (*D*) 10 μm.

porary hypothesis (61), that kinetochores nucleate their associated K-MTs, is supported by drug recovery (7, 70) and in vitro MT growth studies (e.g., 30, 65). By contrast, the older hypothesis (69), that K-MTs are derived from the centrosome, is supported, for example, by the behavior of prometaphase chromosomes in diatom spindles (45, 46, 66), by the finding that within a half-spindle K-MTs have the same growth polarity as centrosomal MTs (8), and by the observation that kinetochores on isolated chromosomes bind centrosome-nucleated MTs in vitro (31). The controversy is further heightened by recent tubulin microinjection experiments that indicate that prometaphase and metaphase kinetochores appear to be the primary sites of K-MT subunit addition and deletion (32) but "probably do not act as independent nucleation sites" (11). Ultrastructural studies of forming K-Fibers (e.g., 5, 33, 34, 51, 54) have been unable to resolve this conflict since, by convention, an MT only becomes a K-MT after it terminates in the kinetochore and it is not possible to determine a priori whether an MT terminating in the kinetochore originated from the kinetochore or the centrosome.

Our IMF and ultrastructural results clearly demonstrate that kinetochores on nonattached NP chromosomes do not nucleate MTs even though they reside, sometimes for several hours, in an experimentally unperturbed mitotic cytoplasm that promotes centrosomal MT assembly. Rather, the first MT to appear at an attaching NP kinetochore traverses the entire distance between the polar region and the kinetochore and often extends well past the kinetochore. The fact that this single MT extends from the polar region often to a point well past the kinetochore (Fig. 11) indicates that it is of centrosomal origin. We therefore conclude that K-MTs in NPs are derived from centrosome-nucleated MTs that grow into, or grow past and then interact laterally with, the corona material of the kinetochore. The mitotic centrosome, which is thought to continuously and randomly probe the cytoplasm with a radial array of growing (and shrinking) MTs (29, 58), can therefore be envisioned to be analogous to a stationary "fisherman" who casts radially about in search of fish in the surrounding water. As with chromosomes in NPs, hungry fish not within the range of the casts will not be caught until either the fisherman moves closer to the fish or the fish wanders closer to the fisherman. Our data indicates that the "casting" range of the NP centrosome is seldom >50 μm.

Our finding, that K-MTs are derived from the spindle pole, provides a straightforward explanation for various light and electron microscopic observations on mitotic cells including, but not limited to, (*a*) the K-MT labeling pattern seen in prometaphase PtK_2 cells fixed shortly after microinjection with *Paramecium* axonemal tubulin (11); (*b*) why chromosomes in sea urchin oocytes do not organize a spindle in the absence of centrosomes (62); (*c*) why the distal kinetochores on monooriented chromosomes in vertebrate cells invariably lack MTs (for reviews see 50, 56); (*d*) the origin of syntelic malorientation and how a kinetochore in various cell types can be attached at any one time to both spindle poles (12, 33, 40); and (*e*) the "proximity" effect, in which the order of chromosome attachment to the forming spindle is influenced by proximity to a centrosome (51, 55).

The conclusion that K-MTs in NPs are derived from the centrosomes appears to be in conflict with reports that chromosomes can organize a spindle in the absence of centrosomes (as in *Pales ferrugenia* spermatocytes; 64) or when removed from the spindle and placed in the cytoplasm adjacent to the main spindle (as in *Drosophila* spermatocytes; 6). However, unlike the mitotic cytoplasm of vertebrate somatic cells, the cytoplasm of spermatocytes frequently contains an ample supply of nonspindle MTs (6, 19), of centrosomal origin, that may associate with kinetochores to form functional spindles.

The interaction of a single centrosomal MT with a kinetochore on an unattached chromosome suffices to attach the chromosome to the spindle and initiate poleward chromosome motion (this study; see also 39). We find that this attachment can occur in NPs even when the kinetochore is not oriented towards a pole (Fig. 11). Thus, kinetochore orientation is not a prerequisite for, but is a consequence of, attachment. Our results further indicate that once a chromosome becomes attached to the spindle, additional astral MTs are

rapidly incorporated into the forming K-Fiber as the chromosome moves poleward (i.e., toward a region of progressively higher MT density). During this time, most of the kinetochore-associated MTs do not terminate in the kinetochore but pass through or graze the corona material. Similar observations concerning the distribution of MTs in forming K-Fibers have been reported for other cell types with astral spindles (e.g., PtK [51], *Drosophila* spermatocytes [5, 14], *Pales* spermatocytes [63]), and even fully formed metaphase K-Fibers contain a variable number of MTs that pass into the chromosome at the periphery of the kinetochore (3, 24, 48).

Once a centrosome-nucleated MT associates with a kinetochore, it becomes more stable to treatments that disrupt non-K-MTs (for review see 56). It is currently unclear whether this increased stability is limited to only those NP K-MTs that actually terminate on the kinetochore plate, as appears to be the case for PtK cells (2, 49), or whether those MTs that graze or pass through the corona material are also similarly stable.

The Mechanism of Prometaphase Chromosome Movement

The initial monopolar attachment of a chromosome is a normal and prevalent feature of vertebrate cell mitosis. Indeed, spindle formation within the same population of cells can occur via several different routes, all of which involve the initial monoorientation of at least some chromosomes (1, 25, 52). In PtK and NPs, a bipolar spindle is rapidly constructed when the spindle poles separate near the time of NEB. Under these conditions, chromosomes positioned closer to a spindle pole usually form an initial monopolar attachment to that pole before achieving a bipolar attachment (34, 50, 51, 53). Alternatively, when the poles are transiently delayed in their separation at the time of NEB, a monopolar spindle is formed as an intermediate pathway to bipolar spindle formation. In these cases, all of the chromosomes form an initial monopolar attachment to the single spindle pole. Finally, when the poles are well separated at the time of NEB, an anaphase-like prometaphase figure is generated in which each chromosome forms a monopolar attachment to one or the other pole. In these situations, the two half-spindles and their monooriented chromosomes may ultimately fuse to form a normal bipolar spindle (1, 48, 52).

The behavior of a prometaphase chromosome during the process of monoorientation is the same regardless of the route by which the spindle is formed. Upon attachment, the chromosome is rapidly transported poleward after which time it undergoes conspicuous oscillatory movements toward and away from the pole (1, 53, 55). Kinetic analyses of poleward chromosome motion after attachment in NPs reveal that chromosome velocity varies widely during transit to the pole, but rates of 25–55 μm/min are not unusual (our Fig. 6 *G* and Fig. 11 *G*; also Alexander, S. P., and C. L. Rieder, manuscript in preparation). Although seldom emphasized and often overlooked, similarly rapid rates of prometaphase chromosome motion have been reported during monoorientation in other types of cells including *Acheta* spermatocytes (up to 24 μm/min; 47), PtK (23 μm/min; 55), and diatoms (150 μm/min; 66). These movement rates are much faster than those of congressing chromosomes in the same systems (34, 44, 55, 66) in which sister kinetochores are thought to be experiencing antagonistic pulling forces from opposite spindle poles. They are also significantly faster than the movement rates exhibited by reattaching grasshopper spermatocyte chromosomes, which usually rapidly reconnect to both spindle poles (35, 39, 40).

With the exception of short and transient oscillatory movements, chromosome motion during mitosis is always directed towards a pole: monooriented prometaphase chromosomes and anaphase chromosomes immediately initiate movement towards the pole to which they are connected, while congressing prometaphase chromosomes move between the spindle poles (but always towards a pole). A major emphasis of mitosis research has therefore been to explain the molecular mechanism(s) behind this poleward movement. For practical reasons (see introduction), most models of chromosome movement are based on data obtained from metaphase and anaphase cells and focus on explaining the relatively slow movements of anaphase chromosomes. Unfortunately, few of these models consider data from prometaphase cells as a starting point for explaining force production within the spindle.

The behavior of diatom chromosomes in vivo, and corresponding ultrastructural studies, prompted Tippit et al. (66; see also 45) to hypothesize that the diatom kinetochore moves along the surface of astral MTs during early prometaphase. However, Tippit et al. (66) found that at least one MT terminated on each of the kinetochores that they analyzed. As a result, they were unable to differentiate whether the force for chromosome movement was generated in association with that single MT terminating in the kinetochore, whether it was derived from those MTs associated laterally with the kinetochore, or both. By contrast, our results clearly demonstrate that an attaching NP chromosome can be rapidly transported poleward along the surface of a single astral MT (Figs. 7, 8, and 11). From this observation, we can conclude that the motor(s) for chromosome movement must be either on the surface of the kinetochore (i.e., within the corona but not within the kinetochore plate), distributed along the surface of K-MTs, or both. Clearly, the mechanism behind this movement is not consistent with models of mitotic force production based on MT subunit treadmilling (22) or MT disassembly (e.g., 18, 20), which include those recently proposed "pac-man" models that couple MT depolymerization to force production (for reviews see 10, 37, 56). In NPs, chromosome movement can occur along the surface of an MT and at a faster rate than that reported for the depolymerization of interphase NP MTs in vivo (17 μm/min; 4) or MTs grown in vitro (e.g., 10–20 μm/min; 30, 68).

The 10–150 μm/min velocity at which vesicles move into the centrosome during saltatory motion in newt eosinophils is inversely correlated with particle size (Hard, R., personal communication). Thus, as in diatoms (45), the peak poleward velocities exhibited by the (extremely) large chromosomes in NPs during monoorientation (up to 55 μm/min; Alexander, S. P., and C. L. Reider, manuscript in preparation) are comparable with the velocities exhibited by large vesicles during transport toward the centrosome. Since both of these movements occur in association with the surface of an MT, it is reasonable to propose that both are produced by the same force-generating mechanism.

Recently, Paschal and co-workers (42, 43) have isolated a cytoplasmic dynein that appears to be the motor responsible for retrograde vesicle transport along MTs. In vitro, this molecule moves MTs (and thus presumably vesicles; see 13) at

speeds of 12–75 μm/min, rates that are comparable with those seen during the poleward translocation of a monooriented chromosome in NPs, PtK, *Acheta* spermatocytes, and diatoms (47, 55, 66). It is therefore possible that the fibrous corona material binds (dynein-like?) motor molecules before or upon interacting with an MT and that once this corona–MT association is established, the kinetochore and its attached chromosome is rapidly transported poleward. In this respect, it is relevant that (*a*) the molecules for prometaphase force production are not located within the kinetochore plate (our conclusion; see above); (*b*) the corona material, which covers the surface of the kinetochore plate, must be the first kinetochore component to interact with spindle MTs; (*c*) a single MT interacting with the corona can support chromosome movement without terminating on the kinetochore plate (our result); and (*d*) the corona appears greatly diminished by metaphase even though it is a very prominent feature of unattached kinetochores (for review see 50). Such a hypothesis would predict that this material is still present during metaphase but that it is much less apparent because it becomes thinly stretched poleward along the surface of K-MTs during K-Fiber formation. This prediction is supported by the observation that in PtK cells the corona, which appears greatly reduced or absent on metaphase kinetochores (50), once again becomes a prominent feature after the kinetochores are depleted of K-MTs by incubation in high concentrations of colcemid (Cassimeris, L., C. L. Rieder, and E. D. Salmon, unpublished observations). When fully stretched, the fibrous corona may be analogous to the "collar" material described for diatoms (44, 46), the kinetochore-associated microfilaments seen in *Oedogonium* (59), and the nonmicrotubular force-producing K-Fiber component predicted by Forer (9, 10).

There are several interesting facets to our model if one assumes that the corona material of sister kinetochores contains approximately equal numbers of force-producing molecule-binding sites. Under this condition, the model would predict that force generation would not be strictly dependent on the number of MTs present at the kinetochore since the same amount of force would be generated when a given number of force-producing sites are dispersed along one, several, or numerous MTs. The distal (nonattached) kinetochore of a monooriented chromosome would therefore not be expected to initiate congression upon interacting with a single (long) MT originating from the distal pole because the force generated in association with this single K-MT would be no greater than, and probably much less than, the opposing force generated by the kinetochore attached to the nearer pole. However, each chromatid of a congressing chromosome is influenced by two antagonistic forces: one generated by the K-Fiber that is directed towards the pole to which the kinetochore is attached and another, generated by the pole, which is directed against the chromosome (53, 57). It is this latter aster elimination or ejection force, which is hypothesized to decrease with increasing distance from the spindle pole (57), that is envisioned in our model to be responsible for chromosome congression to the metaphase plate. The addition and deletion of K-MT subunits at the kinetochore (32), produced by tension (e.g., 17, 36) on the chromosome generated by antagonistic antipolar forces originating from the asters, would allow MTs terminating at sister kinetochores to elongate and shorten during congression movements. That the antipolar forces produced by the asters are of sufficient magnitude to produce congression is suggested by the observation that a monooriented chromosome can slowly congress to the metaphase plate in the apparent absence of activity at its distal kinetochore (34). Furthermore, the average length of a bipolar metaphase NP half-spindle, which is equivalent to the final congression position of a metaphase chromosome, is 22 μm (48), approximately the same distance from the pole that a monopolar chromosome initially becomes positioned (Figs. 1, 4, and 11; see also 53) in the absence of K-MTs on the distal kinetochore.

In our model of congression, multivalent chromosomes (e.g., produced by gamma-irradiation of grasshopper nymphs; 16) would be expected to achieve a final congression position closer to the pole that was attached to the greater number of kinetochores. However, this position would not necessarily result because the magnitude of the poleward traction force along a K-Fiber is directly proportional to the length of the fiber (or the MTs within the fiber, as suggested in reference 16). Rather, it would result because the additional kinetochores on one side of the metaphase plate provide a proportionally greater number of force-producing sites to counter the aster ejection force within that half-spindle. The final congression position of such chromosomes would therefore represent that point where the poleward forces on the chromosome are balanced by the polar ejection forces: i.e., the length of a K-Fiber would be the result, but not the cause, of congression. Destroying part of a metaphase kinetochore by laser microsurgery would be expected to result in movement of the chromosome closer to the pole facing the undamaged kinetochore not because the number of K-MTs is reduced on the damaged kinetochore (for review see 56) but because the number of force-producing sites associated with this kinetochore is reduced.

Nicklas (36, 38) has recently determined that the maximum forces acting on prometaphase and anaphase chromosomes in the grasshopper spermatocyte are about the same (1×10^{-5} vs. 7×10^{-5} dyne, respectively) and that this is significantly greater than the force required to overcome viscous resistance to move a chromosome poleward during anaphase (10^{-8} dyne). The observation that the maximum force potential of the spindle is nearly 10,000 times greater than that needed for normal chromosome movement suggests that chromosome velocity is "controlled by a governor, a velocity-limiting device or process" (39; see also 10, 38). Our model is consistent with Nicklas's data since it predicts that the motors associated with the kinetochore corona generate the same amount of force during anaphase and prometaphase. Our evidence for a governor is as follows: the forces responsible for the poleward movement of a monoorienting prometaphase chromosome, which can be generated in association with as few as one MT (Figs. 6 and 11), move the chromosome at velocities up to 55 μm/min. By contrast, the forces responsible for the movement of a monooriented chromosome with a fully developed K-Fiber, created in metaphase NPs and PtK cells by completely ablating one kinetochore with a laser, move the chromosome towards the pole that the nonirradiated kinetochore faces with the same slow (2–3 μm/min) speed exhibited by anaphase chromosomes (27; also Rieder, C. L., and E. D. Salmon, unpublished observations). Thus, in the absence of antagonistic pulling forces acting at sister kinetochores, an increase in the number of MTs terminating at the only active kinetochore of a monooriented chromosome correlates with a much slower rate of

chromosome movement. This analysis therefore supports the conclusion that the rate at which an anaphase chromosome moves is limited or governed, perhaps by the disassembly of K-MTs at the kinetochore (for reviews see 10, 36, 38).

Our model, in which force is produced from a motor molecule–mediated interaction between the corona and MT, differs from that of Pickett-Heaps (for review see 44), which postulates that kinetochores attach to some nonkinetochore force-generating spindle component (i.e., the collar) originating from the polar regions that becomes stretched over the MTs. It also differs from those pac-man models of anaphase chromosome movement in which K-MTs are thought to be actively pulled through sleeves in the kinetochore by motor molecules within the kinetochore plate (for reviews see 10, 37, 56). In this respect, our data demonstrate that the force for chromosome movement is not produced within the kinetochore plate (see above) but that it is produced in association with the material extending from the surface of the plate. Our proposal is therefore not subject to those kinetochore/microtubule geometry constraints noted by Nicklas (37) to be inherent in the microtubule-in-a-sleeve models. Rather, it is consistent with the fact that MTs of the forming K-Fiber associate with the kinetochore at various angles (5, 40, 51; Fig. 10). Finally, our proposal shares many similarities with Forer's hypothesis (for review see 10) that the force-producing component/complex is attached to the kinetochore and extends poleward along the spindle fiber. It differs, however, in the nature and origin of the force-producing component and on the degree to which force production is dependent on MTs.

This paper is dedicated to the memory of Alvin Ray Rieder. The authors thank Drs. S. S. Bowser, J. Hayden, and C. A. Mannella for stimulating discussions related to the work presented in this manuscript. We also thank Dr. E. A. Davison, Mr. M. M. Marko, Ms. E. Mandeville, and Ms. T. LaMena for excellent technical help; Dr. L. Binder for providing us with TU-27 antibody against β-tubulin; and Ms. S. Nowogrodzki-Rieder for editorial assistance.

This work was supported in part by National Institutes of Health General Medical Science grant RO1-40198 (to C. L. Rieder) and Biotechnological Resource grant RR 01219 awarded by the Division of Research Resources, Department of Health and Human Services/Public Health Service, to support the Wadsworth Center's Biological Microscopy and Image Reconstruction facility as a National Biotechnological Resource.

Received for publication 7 August 1989 and in revised form 20 September 1989.

References

1. Bajer, A. S. 1982. Functional autonomy of monopolar spindle and evidence for oscillatory movement in mitosis. *J. Cell Biol.* 93:33–48.
2. Brinkley, B. R., and J. Cartwright. 1975. Cold labile and cold stable microtubules in the mitotic spindle of mammalian cells. *Ann. NY Acad. Sci.* 253:428–439.
3. Cassimeris, L., S. Inoue, and E. D. Salmon. 1988. Microtubule dynamics and the chromosomal spindle fiber: analysis by fluorescence and high resolution polarizaton microscopy. *Cell. Motil. Cytoskeleton.* 10:185–196.
4. Cassimeris, L., N. K. Pryer, and E. D. Salmon. 1988. Real-time observations of microtubule dynamic instability in living cells. *J. Cell Biol.* 107:2223–2231.
5. Church, K., and H.-P. P. Lin. 1982. Meiosis in *Drosophila melanogaster*. II. The prometaphase-I kinetochore microtubule bundle and kinetochore orientation in males. *J. Cell Biol.* 93:365–373.
6. Church, K., R. B. Nicklas, and H.-P. Lin. 1986. Micromanipulated bivalents can trigger mini-spindle formation in *Drosphila melanogaster* spermatocyte cytoplasm. *J. Cell Biol.* 103:2765–2773.
7. DeBrabander, M., G. Geuens, J. DeMey, and M. Joniau. 1981. Nucleated assembly of mitotic microtubules in living PtK_2 cells after release from nocodazole treatment. *Cell Motil.* 1:469–484.
8. Euteneuer, U., and J. R. McIntosh. 1981. Structural polarity of kinetochore microtubules in PtK_1 cells. *J. Cell Biol.* 89:338–345.
9. Forer, A. 1969. Chromosome movements during cell division. *In* Handbook of Molecular Cytology. A Lima-de-Faria, editor. North-Holland Publishing Co., Amsterdam. 554–601.
10. Forer, A. 1988. Do anaphase chromosomes chew their way to the pole or are they pulled by actin? *J. Cell Sci.* 91:449–453.
11. Geuens, G., A. M. Hill, N. Levilliers, A. Adoutte, and M. DeBrabander. 1989. Microtubule dynamics investigated by microinjection of *Paramecium* axonemal tubulin: lack of nucleation but proximal assembly of microtubules at the kinetochore during prometaphase. *J. Cell Biol.* 108:939–953.
12. Ghosh, S., and N. Paweletz. 1987. Centrosome–kinetochore interaction in multinucleate cells. *Chromosoma (Berl.).* 95:136–143.
13. Gibbons, I. R. 1988. Dynein ATPases as microtubule motors. *J. Biol. Chem.* 263:15837–15840.
14. Goldstein, L. S. B. 1981. Kinetochore structure and its role in chromosome orientation during the first meiotic division in male *D. melanogaster*. *Cell.* 25:590–602.
15. Gorbsky, G. J., P. J. Sammak, and G. G. Borisy. 1987. Chromosomes move poleward in anaphase along stationary microtubules that coordinately disassemble from their kinetochore ends. *J. Cell Biol.* 104:9–18.
16. Hays, T. S., D. Wise, and E. D. Salmon. 1982. Traction force on a kinetochore at metaphase acts as a linear function of kinetochore fiber length. *J. Cell Biol.* 93:374–382.
17. Hill, T. L., and M. W. Kirschner. 1982. Bioenergetics and kinetics of microtubule and actin filament assembly-disassembly. *Int. Rev. Cytol.* 78:1–125.
18. Inoue, S. 1981. Cell division and the mitotic spindle. *J. Cell Biol.* 91(3, Pt. 2):131s–147s.
19. Janicke, M. A., and J. R. LaFountain, Jr. 1984. Malorientation in half-bivalents at anaphase: analysis of autosomal laggards in untreated, cold-treated, and cold-recovering crane fly spermatocytes. *J. Cell Biol.* 98:859–869.
20. Koshland, D. E., T. J. Mitchison, and M. W. Kirschner. 1988. Polewards chromosome movement driven by microtubule depolymerization in vitro. *Nature (Lond.).* 331:499–504.
21. Marko, M., A. Leith, and D. Parsons. 1988. Three-dimensional reconstruction of cells from serial sections and whole-cell mounts using multilevel contouring of stereo micrographs. *J. Electron Microsc. Tech.* 9:395–411.
22. Margolis, R. L., L. Wilson, and B. Kiefer. 1978. Mitotic mechanism based on intrinsic microtubule behavior. *Nature (Lond.).* 272:450–452.
23. McGee-Russell, S. M., and R. D. Allen. 1971. Reversible stabilization of labile microtubules in the reticulopodial network of Allogromia. *Adv. Cell Mol. Biol.* 1:153–184.
24. McIntosh, J. R., W. Z. Cande, J. Snyder, and K. Vanderslice. 1975. Studies on the mechanism of mitosis. *Ann. NY Acad. Sci.* 253:407–427.
25. McIntosh, J. R., W. Z. Cande, and J. A. Snyder. 1975. Structure and physiology of the mammalian mitotic spindle. *In* Molecules and Cell Movement. S. Inoue and R. E. Stephens, editors. Raven Press, New York. 31–76.
26. McIntosh, J. R., G. P. A. Vigers, and T. S. Hays. 1989. Dynamic behavior of mitotic microtubules. *In* Cell Movement. Vol. 2. Kinesin, dynein, and microtubule dynamics. Alan R. Liss Inc., New York. 371–382.
27. McNeil, P. A., and M. W. Berns. 1981. Chromosome behavior after laser microirradiation of a single kinetochore in mitotic PtK_2 cells. *J. Cell Biol.* 88:543–553.
28. Mitchison, T. J. 1988. Microtubule dynamics and kinetochore function in mitosis. *Annu. Rev. Cell Biol.* 4:527–549.
29. Mitchison, T. J., and M. W. Kirschner. 1984. Dynamic instability of microtubule growth. *Nature (Lond.).* 312:237–242.
30. Mitchison, T. J., and M. W. Kirschner. 1985. Properties of the kinetochore in vitro. I. Microtubule nucleation and tubulin binding. *J. Cell Biol.* 101:755–765.
31. Mitchison, T. J., and M. W. Kirschner. 1985. Properties of the kinetochore in vitro. II. Microtubule capture and ATP-dependent translocation. *J. Cell Biol.* 101:766–777.
32. Mitchison, T. J., L. Evans, E. Schulze, and M. Kirschner. 1986. Sites of microtubule assembly and disassembly in the mitotic spindle. *Cell.* 45:515–527.
33. Mole-Bajer, J. 1975. The role of centrioles in the development of the astral spindle (newt). *Cytobios.* 13:117–140.
34. Mole-Bajer, J, A. Bajer, and A. Owczarzak. 1975. Chromosome movements in prometaphase and aster transport in the newt. *Cytobios.* 13:45–65.
35. Nicklas, R. B. 1967. Chromosome micromanipulation. II. Induced reorientation and the experimental control of segregation in meiosis. *Chromosoma (Berl.).* 21:17–50.
36. Nicklas, R. B. 1983. Measurements of the force produced by the mitotic spindle in anaphase. *J. Cell Biol.* 97:542–548.
37. Nicklas, R. B. 1988. Chromosomes and kinetochores do more in mitosis than previously thought. *In* Chromosome Structure and Function. J.

Perry Gustafson and R. Appels, editors. Plenum Publishing Corp., New York. 53–74.
38. Nicklas, R. B. 1988. The forces that move chromosomes in mitosis. *Annu. Rev. Biophys. Biophys. Chem.* 17:431–449.
39. Nicklas, R. B., and D. F. Kubai. 1985. Microtubules, chromosome movement, and reorientation after chromosomes are detached from the spindle by micromanipulation. *Chromosoma (Berl.).* 92:313–324.
40. Nicklas, R. B., B. R. Brinkley, D. A. Pepper, D. F. Kubai, and G. K. Rickards. 1979. Electron microscopy of spermatocytes previously studied in life: methods and some observations on micromanipulated chromosomes. *J. Cell Sci.* 35:87–104.
41. Nicklas, R. B., G. M. Lee, C. L. Rieder, and G. Rupp. 1989. Mechanically cut mitotic spindles: clean cuts and stable microtubules. *J. Cell Sci.* In press.
42. Paschal, B. M., and R. B. Vallee. 1987. Retrograde transport by the microtubule associated protein MAP 1C. *Nature (Lond.).* 330:181–183.
43. Paschal, B. M., H. S. Shpetner, and R. B. Vallee. 1987. MAP 1C is a microtubule-activated ATPase which translocates microtubules in vitro and has dynein-like properties. *J. Cell Biol.* 105:1273–1282.
44. Pickett-Heaps, J. D. 1986. Mitotic mechanisms: an alternative view. *Trends Biochem. Sci.* 11:504–507.
45. Pickett-Heaps, J. D., and D. H. Tippit. 1978. The diatom spindle in perspective. *Cell.* 14:455–467.
46. Pickett-Heaps, J. D., D. H. Tippit, and K. R. Porter. 1982. Rethinking mitosis. *Cell.* 29:729–744.
47. Rickards, G. K. 1975. Prophase chromosome movements in living house cricket spermatocytes and their relationship to prometaphase, anaphase and granule movements. *Chromosoma (Berl.).* 49:407–455.
48. Rieder, C. L. 1977. An in vitro light and electron microscopy study of anaphase chromosome movements in normal and temperature elevated *Taricha* lung cells. Ph.D. thesis. University of Oregon, Eugene. 294 pp.
49. Rieder, C. L. 1981. The structure of the cold-stable kinetochore fiber in metaphase PtK_1 cells. *Chromosoma (Berl.).* 84:145–158.
50. Rieder, C. L. 1982. The formation, structure, and composition of the mammalian kinetochore and kinetochore fiber. *Int. Rev. Cytol.* 79:1–58.
51. Rieder, C. L., and G. G. Borisy. 1981. The attachment of kinetochores to the pro-metaphase spindle in PtK_1 cells. *Chromosoma (Berl.).* 82:693–716.
52. Rieder, C. L., and R. Hard. 1989. Newt lung epithelial cells: cultivation, use and advantages for biomedical research. *Int. Rev. Cytol.* In press.
53. Rieder, C. L., E. A. Davison, L. C. W. Jensen, L. Cassimeris, and E. D. Salmon. 1986. Oscillatory movements of monooriented chromosomes and their position relative to the spindle pole result from the ejection properties of the aster and half-spindle. *J. Cell Biol.* 103:581–591.
54. Roos, U.-P. 1973. Light and electron microscopy of rat kangaroo cells in mitosis. II. Kinetochore structure and function. *Chromosoma (Berl.).* 41:195–220.
55. Roos, U.-P. 1976. Light and electron microscopy of rat kangaroo cells in mitosis. III. Patterns of chromosome behavior during prometaphase. *Chromosoma (Berl.).* 54:363–385.
56. Salmon, E. D. 1989. Microtubule dynamics and chromosome movement. *In* Mitosis. J. Hayams and B. R. Brinkley, editors. Academic Press Inc., Orlando, FL. 119–180.
57. Salmon, E. D. 1989. Metaphase chromosome congression and anaphase poleward movement. *In* Cell Movement. Vol. 2. Kinesin, dynein, and microtubule dynamics. Alan R. Liss Inc., New York. 431–440.
58. Salmon, E. D., R. J. Leslie, W. M. Saxton, M. L. Karow, and J.R. McIntosh. 1984. Spindle microtubule dynamics in sea urchin embryos: analysis using fluorescein-labeled tubulin and measurements of fluorescence redistribution after laser photobleaching. *J. Cell Biol.* 99:2165–2174.
59. Schibler, M. J., and J. D. Pickett-Heaps. 1980. Mitosis in *Oedogonium*: spindle microfilaments and the origin of the kinetochore fiber. *Eur. J. Cell Biol.* 22:687–698.
60. Schliwa, M., and J. van Blerkom. 1981. Structural interactions of cytoskeletal components. *J. Cell Biol.* 90:222–235.
61. Schrader, F. 1953. Mitosis. Columbia University Press, New York. 170 pp.
62. Sluder, G., and C. L. Rieder. 1985. Experimental separation of pronuclei in fertilized sea urchin eggs: chromosomes do not organize a spindle in the absence of centrosomes. *J. Cell Biol.* 100:897–903.
63. Steffen, W., and H. Fuge. 1985. Three-dimensional architecture of chromosome fibers in cranefly: amphetelic autosomal univalents in late prometaphase. *Cytobios.* 43:199–212.
64. Steffen, W., H. Fuge, R. Dietz, M. Bastmeyer, and G. Muller. 1986. Aster-free spindle poles in insect spermatocytes: evidence for chromosome-induced spindle formation. *J. Cell Biol.* 102:1679–1687.
65. Telzer, B. R., M. J. Moses, and J. L. Rosenbaum. 1975. Assembly of microtubules onto kinetochores of isolated mitotic chromosomes of HeLa cells. *Proc. Natl. Acad. Sci. USA.* 72:4023–4027.
66. Tippit, D. H., J. D. Pickett-Heaps, and R. Leslie. 1980. Cell division in two large pennate diatoms *Hantzschia* and *Nitzschia*. III. A new proposal for kinetochore function during prometaphase. *J. Cell Biol.* 86:402–416.
67. Wadsworth, P., E. Sheldon, G. Rupp, and C. L. Rieder. 1989. Biotin–tubulin incorporates into kinetochore fiber microtubules during early but not late anaphase. *J. Cell Biol.* 109:2257–2266.
68. Walker, R. A., S. Inoue, and E. D. Salmon. 1989. Asymmetric behavior of severed microtubule ends after ultraviolet-microbeam irradiation of individual microtubules in vitro. *J. Cell Biol.* 108:931–938.
69. Wilson, E. B. 1911. The Cell in Development and Inheritance. 2nd Ed. Macmillan Publishing Co., New York. 483 pp.
70. Witt, P. L., H. Ris, and G. G. Borisy. 1981. Origin of kinetochore microtubules in Chinese hamster ovary cells. *Chromosoma (Berl.).* 80:483–505.